Electronic Supplementary Material (ESI) for Dalton Transactions.
This journal is © The Royal Society of Chemistry 2019

Supporting Information

Facile preparation of Ca(II) carboxymethyl cellulose complex with enhanced calcium bioavailability for treatment of osteoporosis

Jun Hai,[a§] Xuan Tan, [b§] Sheng Yang,[c] Fengjuan Chen,[a] Tianrong Li,[a] Xiangliang Yang,[c] Yanhong Zhu[b*] and Baodui Wang[a,*]

[a] State Key Laboratory of Applied Organic Chemistry Lanzhou University and Key Laboratory of Nonferrous Metal Chemistry and Resources Utilization of Gansu Province, Lanzhou University, Lanzhou 730000, China.

[b] National Engineering Research Center for Nanomedicine, College of Life Science and Technology, Huazhong University of Science and Technology, Wuhan 430074, China.

[c] National Engineering Research Center for Nanomedicine, Huazhong University of Science and Technology, Wuhan 430074, China.

§ These two authors contributed equally to this work.

*E-mail: wangbd@lzu.edu.cn; yhzhu@mail.hust.edu.cn.

SUPPLEMENTARY EXPERIMENTS

Calcium solubility Test. 10 μg/mL of CaCMC and $CaCl_2$ were separately dissolved in deionized water, the solutions pH was adjusted to 2.0~8.0. After 2 h incubation at 37 °C, the solutions were centrifuged at 10000g for 10 min. The total calcium amount in the supernatant was determined by ICP.

20 mg of $CaCl_2$ or CaCMC was dissolved in 50 mL distilled water. The pH was adjusted to 2.0 with 1N HCl. 0.5 mg pepsin-HCl digestion was added, the mixture was incubated in a water bath for 2 h at 37°C. After the gastric digestion simulation model, the pH of the solution was regulated to 7.4 by 0.5 M NaOH. Subsequent, a pancreatin-bile salt mixture was added, and incubated for another 2 h. The reaction was stopped by an ice bath for 15 min. Proteases were inhibited by a boiling water bath for 4 min and then cooled in an ice bath. The digested solution was centrifuged at 13500 rpm for 30 min at 4°C. The supernatants were collected for next use.

Cell culture. NIH3T3 and HeLa cells were cultured in DMEM with 10 % (v/v) fetal bovine serum (FBS, Invitrogen) in 5 % CO_2 at 37 ^{0}C. The CCK-8 assay was performed for *in vitro* cytotoxicity of CaCMC, The CaCMC was suspended with PBS. Subsequently, the NIH3T3 and HeLa cell suspension was added. The final CMC concentration was 50 μg/mL. The mixed suspension was seeded into a 96-well flask with 5×10^3 cells per well and incubated for 48 h. Thereafter, 10 μL CCK-8 per well was injected and incubated for 2 h at 37 ℃ under 5% CO_2. The optical density was measured at 450 nm using a microplate reader (Wallac 1420 Victor).

Measurements. FT-IR spectra were achieved by an infrared spectrometer (Nicolet FT-170SX). Morphology of nanocellulose hydrogel was performed by Field-Emission Scanning Electron Microscope (FE-SEM, FEI, Sirion 200). Emission spectra were noted by a Shimadzu RF-5301 spectrophotometer. X-ray photoelectron spectroscopy (XPS) was investigated on a PHI-5702 multifunctional spectrometer using Al Kα radiation. ^{1}H-NMR spectrums were collected on a JEOL ESC 400M instrument. The mechanical properties of the nanocellulose hydrogels were described by a rheometer (AR-1000 TA Instruments). The

mechanical properties of the nanocellulose hydrogels were characterized by a rheometer with a cone and plate geometry (AR-1000 TA Instruments).

Protocol of UV-vis absorption. The UV-vis absorption is spectrophotometry is a physicochemical analysis technique, the principle is based on the light-absorption capacity of a product where light of wavelength λ through a medium absorbing a distance l with incident intensity I_0, and it emerges with an intensity of I. The absorbance at the wavelength solution is expressed in terms of I and I_0 is given by the Beer-Lambert law:

$$A = log_{10}\left(\frac{I_0}{I}\right) = \varepsilon lc.$$

c is the molar concentration of the absorbing species, ε is the molar extinction coefficient of this species to the wavelength λ, and I is the length traveled by the light in the absorbing medium.

According to the data of Fig. S2, ε is 550 L. cm^{-1}. mol^{-1} for DPY. The absorbance of CMC-DPY is 0.016, so calculated as below:

$C_{CMC\text{-}DPY} = A/\varepsilon = 2.9 * 10^{-2}$ mol L^{-1}

Here we used 1 mL (2 wt%) CMC-DPY for the test, so

$C_{CMC} = 0.002/25{,}000 * 10^{-3} = 8 * 10^{-5}$ mol L^{-1}

THE molar ratio $N = C_{CMC\text{-}DPY} V / C_{CMC} V = 362.5$

This means each CMC can bind about 362 DPY molecular.

SUPPLEMENTARY FIGURES AND TABLES

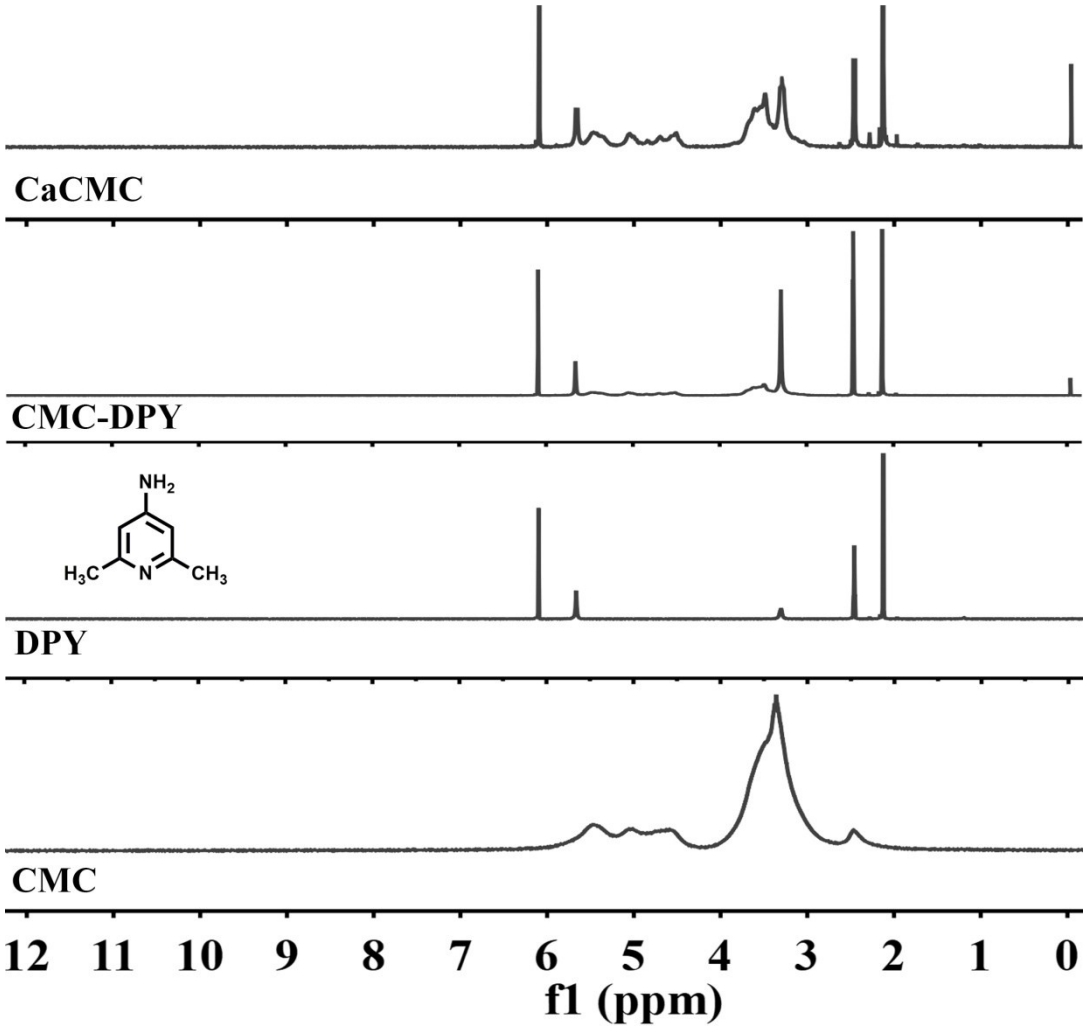

Fig. S1. ^{1}H NMR spectra of CMC, DPY, CMC-DPY and CaCMC in DMSO-d_6.

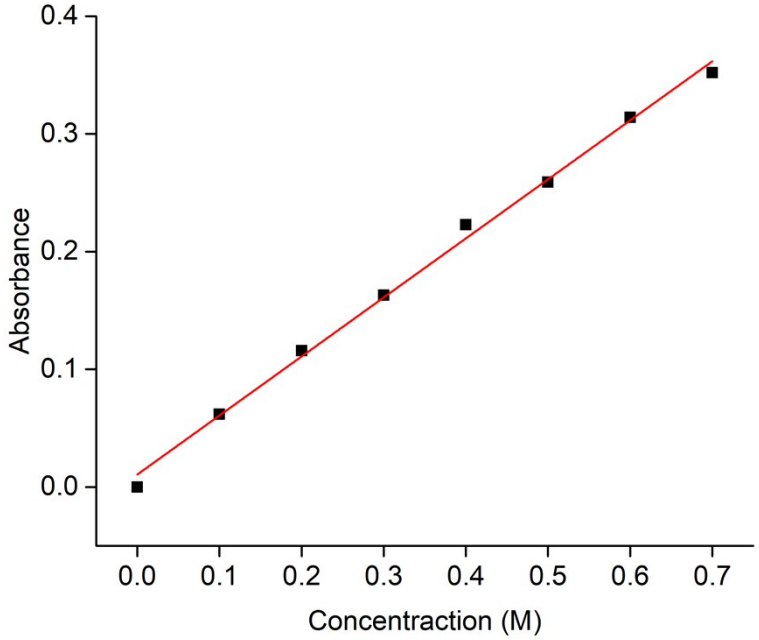

Fig. S2. Plot of the absorbance against the concentration of DPY.

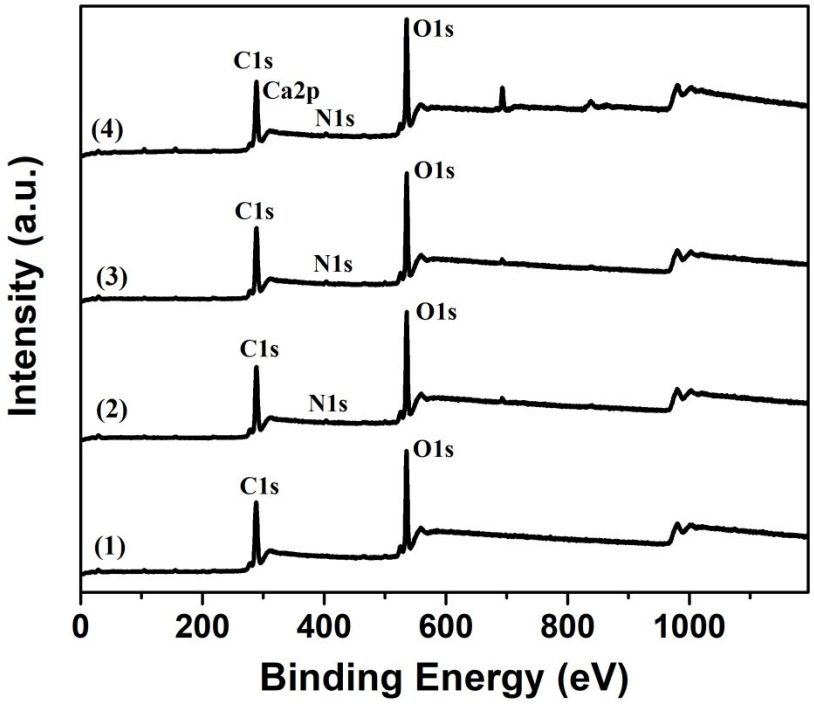

Fig. S3. XPS spectra of (1), (2), (3) and (4).

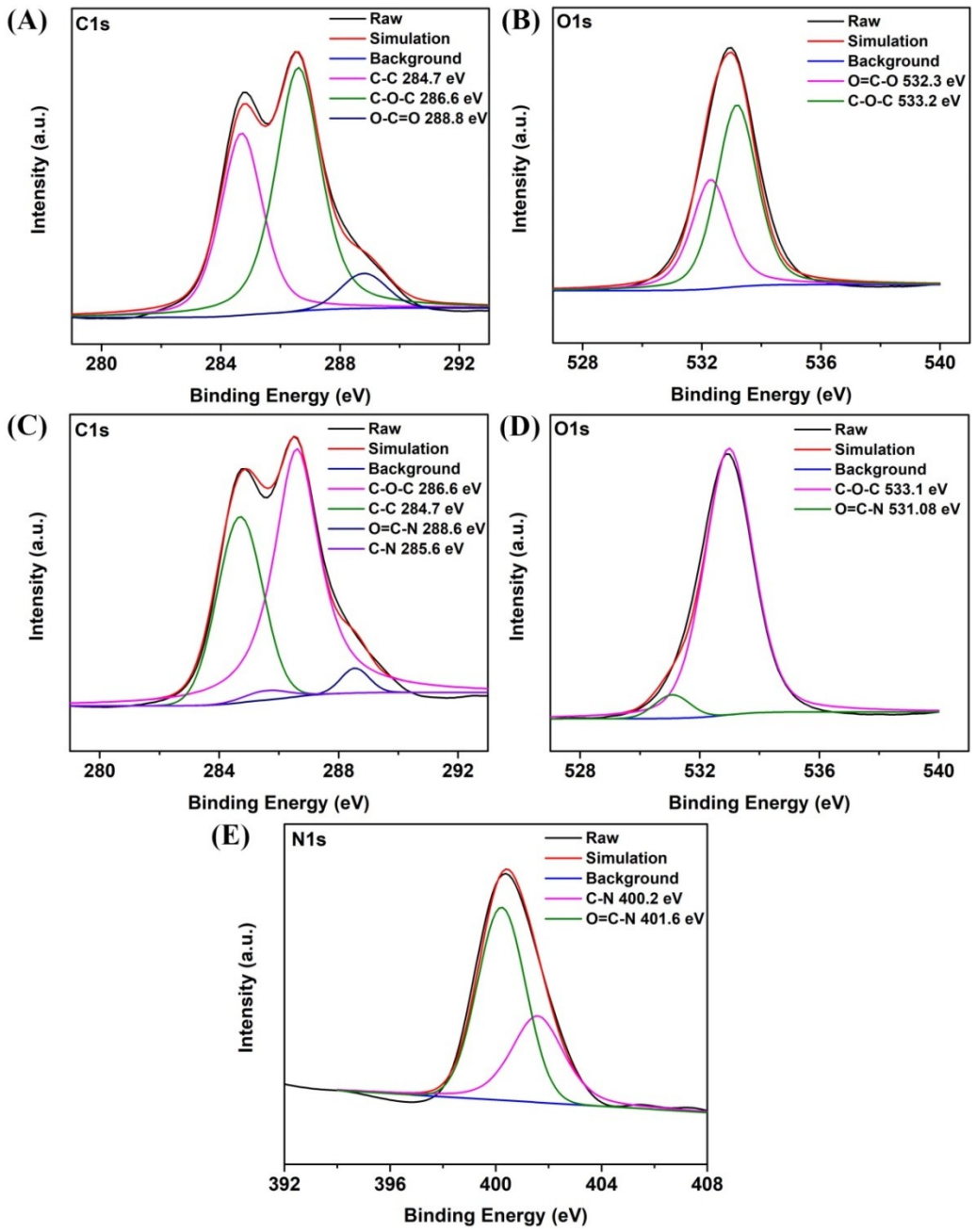

Fig. S4. High-resolution of C1s and O1s XPS spectra of CMC (**A, B**), and C1s, O1s and N1s XPS spectra of CMC-DPY (**2**) (**C-E**).

Fig. S4 shown the C1s spectrum of CMC and CMC-DPY have the same peaks at 284.7, 286.6, and 288.8 eV assigning to C-C/C=C, C-O-C, and O-C=O species, which belong to pyran ring, and carboxyl species. Except for CMC-DPY, the decomposed peak at 288.6 eV belongs to O=C-N in C1s spectrum, the decomposed peak at 531.08 eV belongs to O=C-N in O1s spectrum, and the decomposed peak at 401.6 eV belongs to O=C-N in N1s spectrum, proving the formation of amide bond.

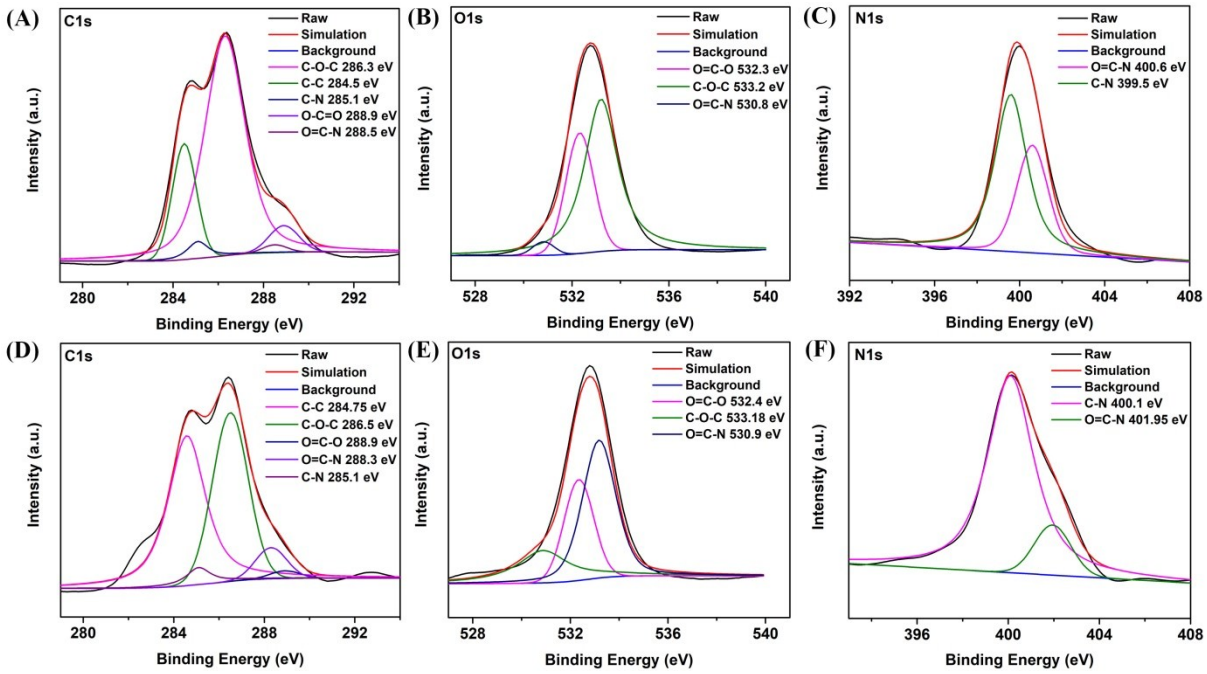

Fig. S5. High-resolution of C1s and O1s XPS spectra of (**3**) (**A-C**), and C1s, O1s and N1s XPS spectra of (**4**) (**D-F**).

As shown in Fig. S5, the C1s spectrum of CMC composite can be decomposed into three main peaks at 284.7, 286.6, and 288.8 eV assigning to C-C/C=C, C-O-C, and O-C=O species, which belong to pyran ring, and carboxyl species. For (**3**), the decomposed peak at 288.5 eV belongs to O=C-N in C1s spectrum (Figure S4A), the decomposed peak at 530.8 eV belongs to O=C-N in O1s spectrum (Figure S4B), and the decomposed peak at 400.6 eV belongs to O=C-N in N1s spectrum (Figure S4C), which proving the formation of amide bond. For CaCMC, the decomposed peak of O=C-N at 288.3 eV in C1s spectrum, 530.9 eV in O1s spectrum and 401.9 eV in N1s spectrum. Since the coordination of Ca^{2+} with O and N, this caused the upshift of the O1s and N1s spectrum for CaCMC.

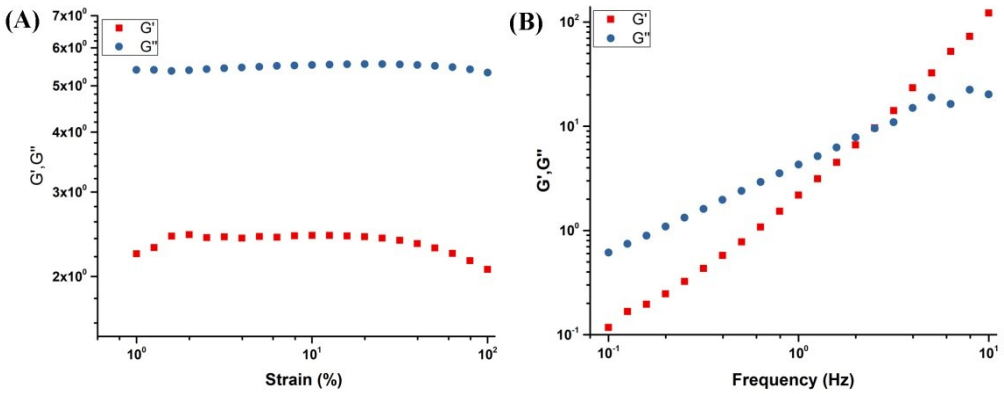

Fig. S6. Variation of storage modulus, G', and loss modulus, G'', in strain-sweep **(A)** and frequency-sweep **(B)** experiments of CaCMC hydrogel at 2 wt%.

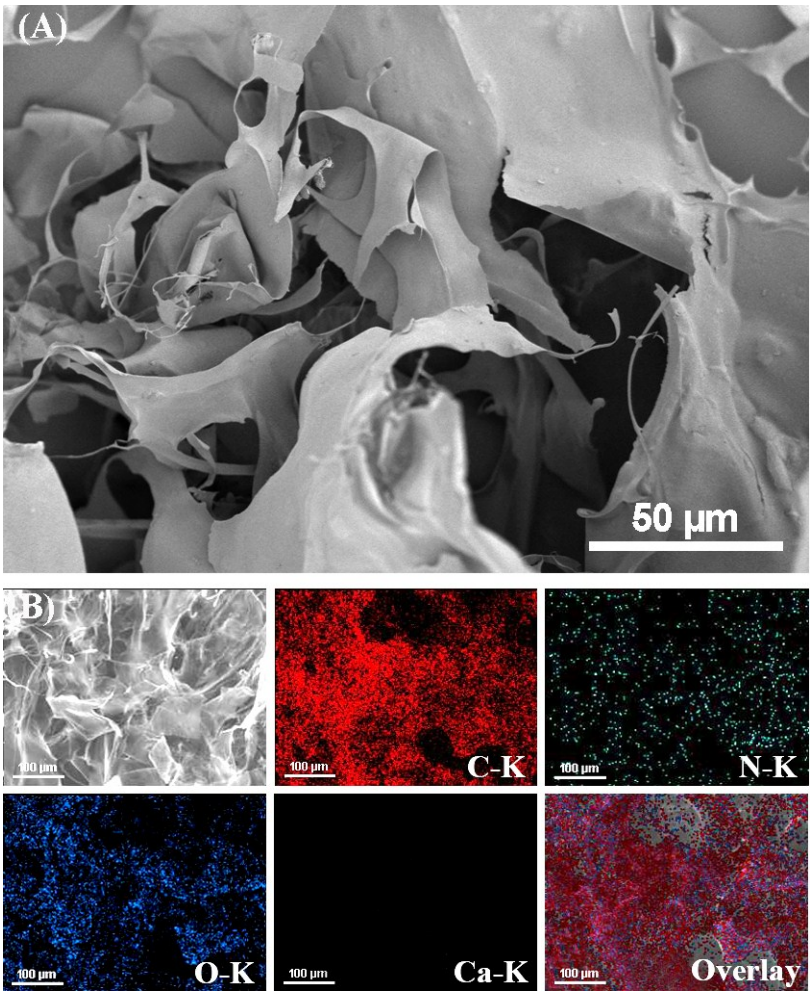

Fig. S7. **(A)** SEM images of CMC-DPY, **(B)** Dark field of STEM and element mapping images of CMC-DPY.

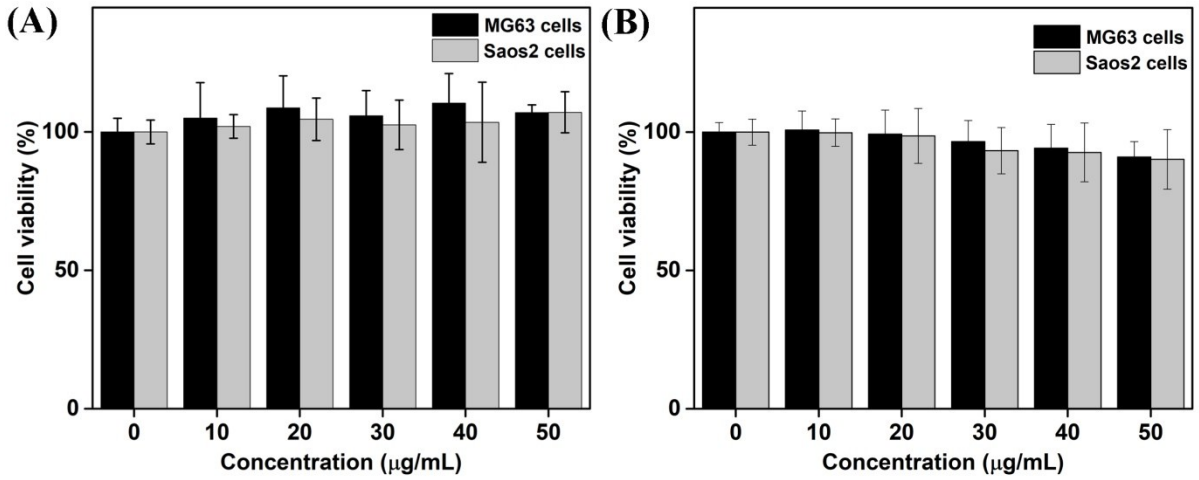

Fig. S8. Cytotoxic assay of CaCMC and CMC-DPY in MG63 and Saos2 cells.

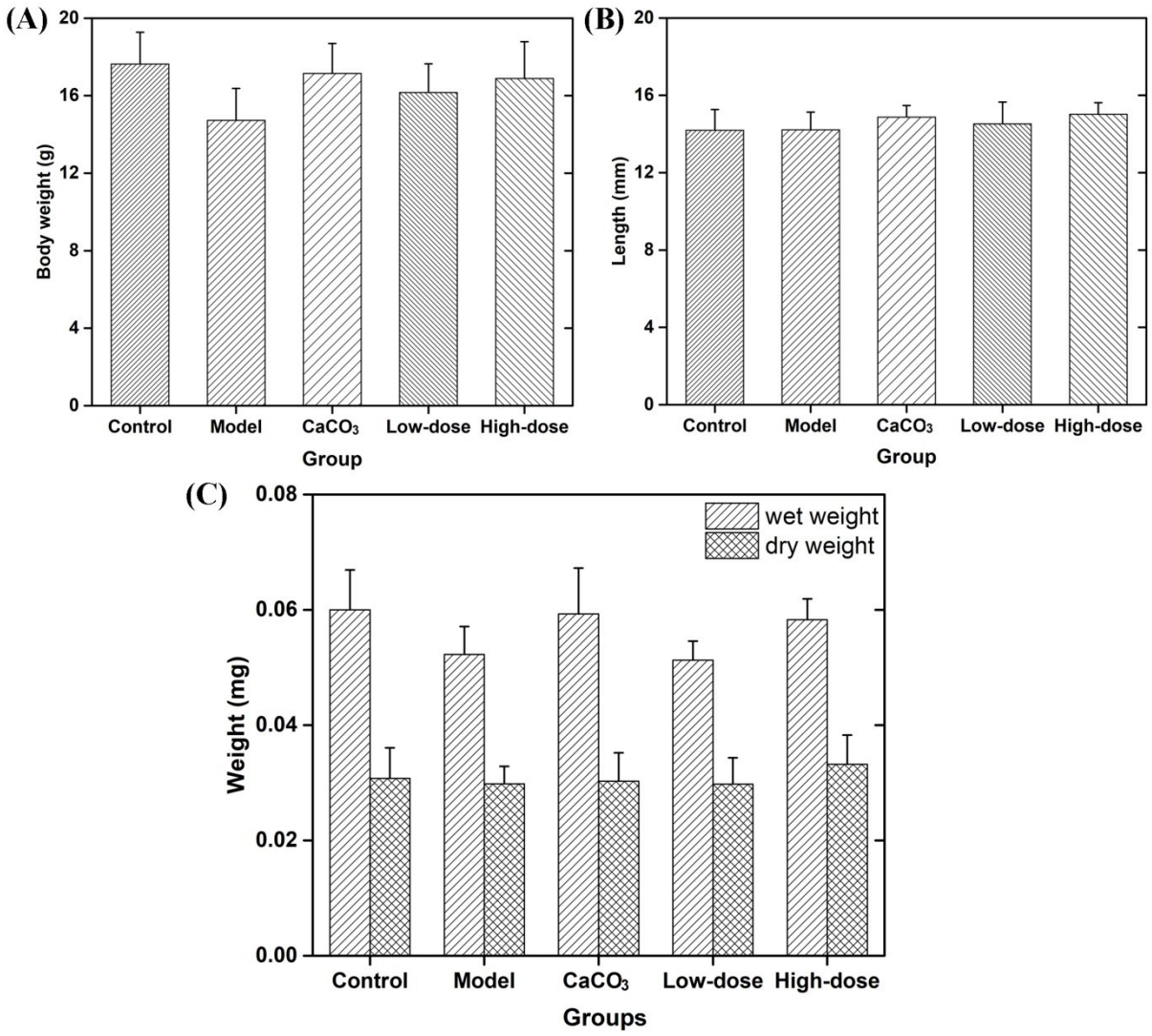

Fig. S9. Metrology index of **(A)** body weight, **(B)** length of the femur, and **(C)** femur weight.

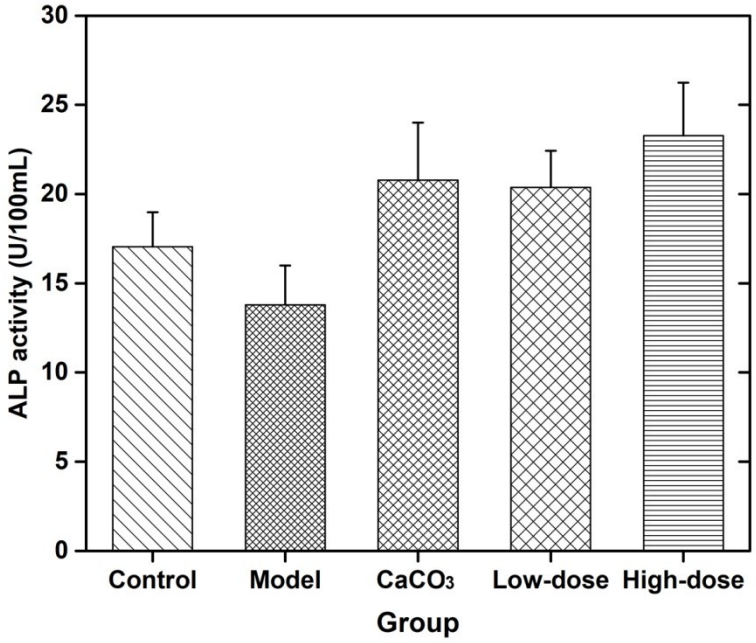

Fig. S10. ALP activity in the serum.

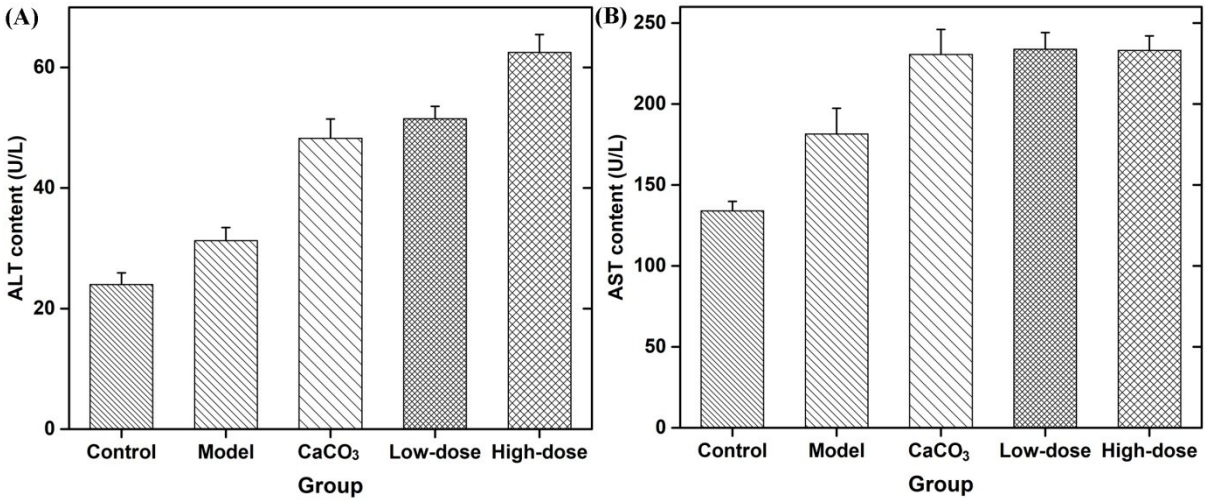

Fig. S11. The content of **(A)** ALT and **(B)** AST in serum.

Table 1. Micro-CT parameter of BMD, BV/TV, Tb.N, Tb.Th, Tb.Sp.

Group	BMD (g/cm^3)	BV/TV (%)	Tb.Th (mm)	Tb.N (1/mm)	Tb.Sp (mm)
Control	0.071	4.98	0.125	0.373	0.780
Model	0.057 ↓	3.77 ↓	0.108 ↓	0.337 ↓	0.964 ↑
$CaCO_3$	0.064	4.64	0.119	0.354	0.907
Low-dose	0.068	4.68	0.116	0.344	0.737
High-dose	0.075 ↑	8.36 ↑	0.135 ↑	0.691 ↑	0.446 ↓